

## Development of an EAM potential for simulation of radiation damage in Fe–Cr alloys

J. Wallenius<sup>a</sup>, I.A. Abrikosov<sup>b,1</sup>, R. Chakarova<sup>a</sup>, C. Lagerstedt<sup>a,\*</sup>,  
L. Malerba<sup>c</sup>, P. Olsson<sup>b</sup>, V. Pontikis<sup>d</sup>, N. Sandberg<sup>a,2</sup>, D. Terentyev<sup>c</sup>

<sup>a</sup> Department of Nuclear and Reactor Physics, Royal Institute of Technology, Alba Nova University Centre, SE-106 91 Stockholm, Sweden

<sup>b</sup> Department of Neutron Research, Angstrom Laboratory, Uppsala University, Box 525, SE-751 20 Uppsala, Sweden

<sup>c</sup> SCK-CEN, Reactor Materials Research Unit, Boeretang 200, 2400 Mol, Belgium

<sup>d</sup> Centre d'Etudes de Chimie Metallurgique, CNRS-UPR2801, 15 rue Georges Urbain, F-94407 Vitry-sur-Seine, France

### Abstract

We have developed a set of EAM potentials for simulation of Fe–Cr alloys. By relaxing the requirement of reproducing the pressure–volume relation at short distances and by fitting to the thermal expansion coefficients of Fe and Cr, stability of the  $\langle 110 \rangle$  self-interstitial could be obtained. For Cr, properties of the paramagnetic state were applied, providing a positive Cauchy pressure. Mixed Fe–Cr pair potentials were fitted to the calculated mixing enthalpy of ferromagnetic Fe–Cr. Simulation of thermal ageing in Fe–Cr alloys using the Fe–20Cr potential exhibited pronounced Cr-precipitation for temperatures below 900 K, a feature not observed at any temperature using a potential fitted to the mixing enthalpy of Fe–5Cr.

© 2004 Elsevier B.V. All rights reserved.

### 1. Introduction

An improved understanding of the radiation effects in ferritic steels is of importance for development of new reactors and maintenance of already operating systems. In order to study defect production and evolution on a short time scale molecular dynamics may be applied. This requires development of adequate many-body potentials. Until recently it was thought that Cr could not be described by ordinary EAM or FS-potentials without angular terms. The present authors have however demonstrated [1] that the elastic constants of

paramagnetic chromium, having a positive Cauchy pressure, may be reproduced by a central potential. Further, the mixing enthalpy of the alloy, which was measured to be strictly positive in the paramagnetic regime, has been shown to be negative for the ferromagnetic state when the Cr concentration is below 6% [2]. In the present contribution, we will dwell on some of the details in the procedure to obtain physically consistent EAM potentials for Fe–Cr that have not previously been published [1]. First, we discuss peculiarities of the thermal expansion data for Cr used for the fit. Then we illustrate the method for obtaining the EAM embedding functions. Finally we describe results from simulation of thermal ageing.

### 2. Construction of the potentials

The embedded atom method (EAM) formalism [3,4] was used to obtain the potentials [1]. The fitting procedure was performed in several steps. The pair potentials

\* Corresponding author. Address: Department of Nuclear and Reactor Physics, SCFAB, KTH, SE-106 91 Stockholm, Sweden. Tel.: +46-8 5537 8193; fax: +46-8 5537 8465.

E-mail address: [christina@neutron.kth.se](mailto:christina@neutron.kth.se) (C. Lagerstedt).

<sup>1</sup> Present address: NTNU, Institutt for fysikk, 7491 Trondheim, Norway.

<sup>2</sup> Present address: Linköpings Universitet, SE-581 83 Linköping, Sweden.

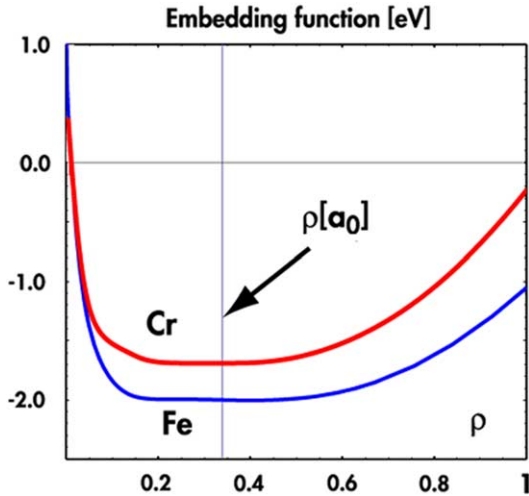


Fig. 1. Embedding functions for Fe and paramagnetic Cr obtained by introducing a cut-off in the Rose expression [5].

of the pure elements for  $R > 2.4 \text{ \AA}$  was obtained by fitting to the lattice parameter, cohesive energy, vacancy formation energy and elastic constants as measured at zero Kelvin. In the case of Cr, the elastic constants of paramagnetic Cr at  $T > 600 \text{ K}$  were linearly extrapolated to zero Kelvin. The embedding functions shown in Fig. 1 were then calculated using this pair potential. We emphasize that a cut-off in the Rose expression [5] had to be introduced to obtain an acceptable second derivative of the embedding functions. The cut-off was made according to the procedure described by Voter [4].

After fixing the embedding function, the pair potential for  $2.0 \text{ \AA} < R < 2.4 \text{ \AA}$  was determined by fitting to temperature dependent lattice parameters of Fe and artificial Cr data, identical to that of paramagnetic Cr-5V [6,7]. In Fig. 2 we display the temperature dependence of the thermal expansion coefficients of Cr and Cr-5V, adapted from [7]. Note that it is sufficient to add a few percent of iron or vanadium to make a Cr based alloy paramagnetic even at room temperature [7,8]. For the short range of the pair potentials, a smooth transition to the universal Coulomb function of Biersack was made [9]. Details of the pair potentials, including range parameters and spline coefficients can be found in Ref. [1].

The cross potentials for the alloy were obtained by fitting to the mixing enthalpy of ferromagnetic Fe-Cr calculated with the EMTO method [2]. Previous attempts to construct mixed pair potentials for Fe-Cr [10,11] relied on fitting to the mixing enthalpy of the paramagnetic state of the alloy, which is strictly positive. A single pair-potential for the Fe-Cr interaction would not easily reproduce the change in sign of the formation energy of the relevant magnetic state. Therefore, a set of

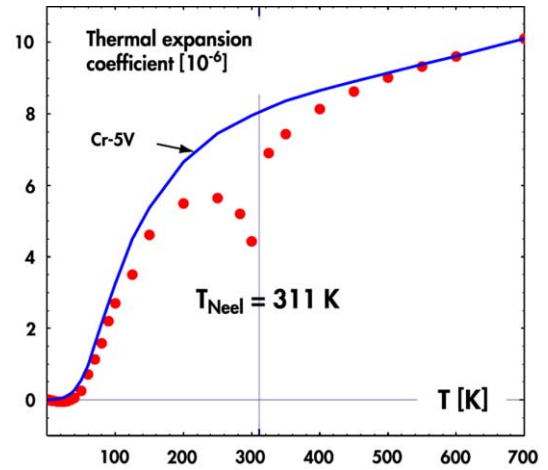


Fig. 2. Thermal expansion coefficients of Cr and paramagnetic Cr-5V, adapted from [7]. Note the cusp for pure Cr at the Néel temperature.

potentials has been created, providing the correct total energy of the random ferromagnetic alloy.

### 3. Verification and discussion

#### 3.1. Thermodynamic properties and point defects

The first test any new potential should be subjected to is if it reproduces experimental thermodynamical properties. The second test is the properties of point defects. We have used the molecular dynamics (MD) code DYMOKA [12] to calculate formation, binding, migration, activation and substitutional energies of different objects. The results are presented in Table 1 together with values calculated using potentials from literature as well as experimental data.

The iron potential of Ackland et al. has been considered as state-of-the-art. Comparing with properties calculated using our potential we note that they yield similar structural properties, but that the thermal expansion predicted by Ackland appears to be unphysical. The largest experimental uncertainty is seen to be in the formation energies of vacancies and interstitials and this is also where our potential diverges the most from the other potentials. For the formation energy of a vacancy we have quoted the latest experiments [20] for high purity iron. We further note that very recent ab initio calculations yield a vacancy formation energy differing by less than 0.05 eV from our value [21]. The predicted value of 7.72 eV for the formation energy of interstitials in Fe is quite different from the 4.9 eV fitted by Ackland. Experimentally the situation is unclear since there is such a large discrepancy between electron

Table 1  
Properties of the new potential

| Fe  | This work | Exp.                   | Ackland                |        |
|---|-----------|------------------------|------------------------|--------|
| $B$   | 172       | 173 <sup>a</sup>       | 178                    |        |
| $C'$  | 56.7      | 52.5 <sup>a</sup>      | 49.0                   |        |
| $C_{44}$                                      | 135       | 122 <sup>a</sup>       | 116                    |        |
| $E_{\text{coh}}$                              | 4.28      | 4.28                   | 4.316                  |        |
| $E_{\text{bcc}} - E_{\text{fcc}}$             | -0.047    | -0.050 <sup>b</sup>    | -0.054                 |        |
| $E_{\text{vac}}^{\text{SD}}$                  | 2.91      | 2.91 <sup>c</sup>      | 2.48                   |        |
| $E_{\text{vac}}^{\text{f}}$                   | 2.04      | 2.0 ± 0.2 <sup>d</sup> | 1.62                   |        |
| $E_{(110)}^{\text{f}}$                        | 7.72      | 3-12 <sup>e</sup>      | 4.87                   |        |
| $E_{(110)}^{\text{f}} - E_{(111)}^{\text{f}}$ | -0.23     | -0.30 <sup>f</sup>     | -0.12                  |        |
| $\alpha$ ( $T = 300$ K)                       | 12.8      | 11.7 <sup>g</sup>      | 7.4                    |        |
| $\alpha$ ( $T = 600$ K)                       | 14.2      | 15.8 <sup>g</sup>      | 7.2                    |        |
| Cr  | This work | Exp. (AFM)             | Exp. (PM)              | Farkas |
| $B$   | 207       | 195 <sup>h</sup>       | 207 <sup>h</sup>       | 148    |
| $C'$  | 153       | 153 <sup>h</sup>       | 155 <sup>h</sup>       | 42.5   |
| $C_{44}$                                      | 105       | 104 <sup>h</sup>       | 105 <sup>h</sup>       | –      |
| $E_{\text{coh}}$                              | 4.10      | 4.10                   | 4.10                   | 4.10   |
| $E_{\text{bcc}} - E_{\text{fcc}}$             | -0.025    | –                      | –                      | -0.053 |
| $E_{\text{vac}}^{\text{SD}}$                  | 2.93      | –                      | 2.95 <sup>i</sup>      | 2.30   |
| $E_{\text{vac}}^{\text{f}}$                   | 2.14      | –                      | 2.0 ± 0.2 <sup>j</sup> | 1.12   |
| $E_{(110)}^{\text{f}}$                        | 5.16      | –                      | –                      | 3.03   |
| $E_{(110)}^{\text{f}} - E_{(111)}^{\text{f}}$ | -0.62     | –                      | –                      | 0.19   |
| $\alpha$ ( $T = 300$ K)                       | 7.5       | 4.4 <sup>k</sup>       | 7.9 <sup>k</sup>       | 5.2    |
| $\alpha$ ( $T = 600$ K)                       | 9.8       | –                      | 9.6 <sup>k</sup>       | 9.5    |
| Fe–Cr   | Fe–5Cr    | Fe–20Cr                | VASP                   | Farkas |
| $E_{(110)}^{\text{f}}$                        | 7.63      | 8.19                   | 3.99 <sup>l</sup>      | 4.31   |
| $E_{\text{Cr}}^{\text{f}}$                    | +0.18     | +0.46                  | -0.03 <sup>l</sup>     | +0.70  |
| $E_{(110)}^{\text{b}}$                        | +0.27     | -0.01                  | -0.43 <sup>l</sup>     | +0.05  |
| $E_{(110)}^{\text{f}} - E_{(111)}^{\text{f}}$ | -0.03     | -0.20                  | -0.11 <sup>l</sup>     | +0.07  |

Comparison is made with experimental data, VASP ab initio data [13,14] and other potentials. For Fe we have compared with the potential of Ackland [15]. For Cr there are experiments on both the anti-ferromagnetic (AFM) phase at room temperature as well as the paramagnetic (PM) phase at higher temperatures. The Farkas potential [10] is used as a comparison for pure Cr and the Fe–Cr alloy. For the alloy we have the two new potentials, Fe–5Cr and Fe–20Cr, fitted to different mixing enthalpies.

<sup>a</sup> Ref. [16].

<sup>b</sup> Ref. [17].

<sup>c</sup> Refs. [18,19].

<sup>d</sup> Ref. [20].

<sup>e</sup> Ref. [22,23].

<sup>f</sup> Ref. [23].

<sup>g</sup> Ref. [5].

<sup>h</sup> Ref. [27].

<sup>i</sup> Ref. [28].

<sup>j</sup> Ref. [29].

<sup>k</sup> Ref. [6].

<sup>l</sup> Ref. [14].

and neutron irradiation experiments. The experimental values are derived from measurements of stored energy release per resistivity recovery ( $dQ/d\rho$ ) in samples irradiated at low temperature [23,24]. The enthalpy for formation of a Frenkel pair is obtained by multiplying  $dQ/d\rho$  with an assumed resistivity  $\Omega_F$  for a single

Frenkel pair. Estimates of  $\Omega_F$  vary from 0.20 to 0.30  $m\Omega\text{cm}$  [25,26]. Selecting the higher value, Wollenberger arrives at a formation energy  $E_{(110)}^{\text{f}} = 6.6$  eV for a Frenkel pair in electron irradiated  $\alpha$ -Fe, and  $E_{(110)}^{\text{f}} = 13.6$  eV for a neutron irradiated sample [24]. Subtracting a vacancy formation energy of 2.0 eV would

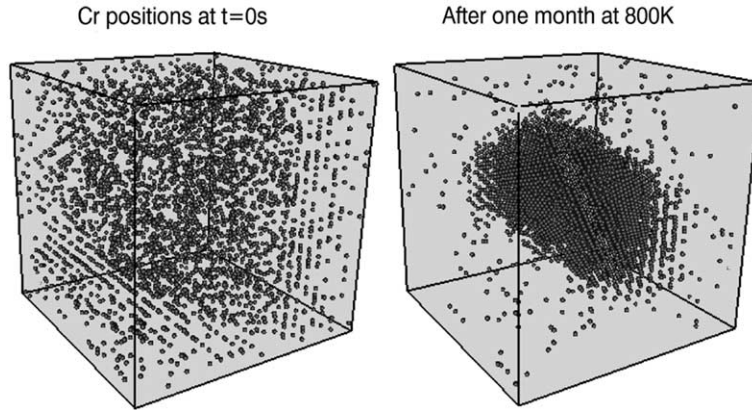


Fig. 3. The distribution of Cr atoms in a box with 16 000 atoms, before and after thermal ageing at 800 K. In total there are 20% Cr atoms in the box. A crystal clear segregation is observed, with the formation of a single cluster.

then give  $E_{(110)}^f = 4.6$  eV in the former case, and 11.6 eV in the latter. The uncertainty of these values is obviously large, since just by assuming  $\Omega_F = 0.20$  m $\Omega$ cm, one could obtain  $E_{(110)}^f = 7.7$  eV for the neutron irradiated sample. Note that results from the electron irradiation are not necessarily more accurate, since experimental boundary conditions are more difficult to control in stages  $I_A$  to  $I_C$  (absent in neutron irradiation) than in stage  $I_D$ .

The SIA formation energy in iron has recently been calculated using ab initio codes as  $E_{(110)}^f = 3.4$  eV [14,21]. This result is compatible with data from electron irradiations. However, since the calculation did not take into account possible effects of non-collinear magnetism, the discrepancy with data from neutron irradiated samples remains an open question.

### 3.2. Chromium precipitation

The well-known 475 °C embrittlement of high-Cr Fe–Cr alloys is due to nano-segregation of chromium. A potential that aims at a correct description of a material should be able to predict such a phase separation. The ranges in which we have this effect are Cr content between 10% and 90% and temperatures between 750 and 900 K [30,31]. We have simulated thermal ageing by introducing a vacancy in the system and letting it exchange places with its neighbours in a kinetic Monte Carlo (KMC) scheme. The frequency for a lattice atom to exchange position with a neighbouring vacancy is

$$\Gamma(T) = \nu C_{\text{vac}}(T) \exp(-E_m/k_B T), \quad (1)$$

where  $\nu$  is the attempt frequency of the jump,  $C_{\text{vac}}$  is the concentration of vacancies and  $E_m$  is the vacancy migration energy. The average time step is then equal to the inverse of  $8\Gamma$ , where eight is the number of nearest neighbours.

This vacancy-assisted migration is assumed to be the driving force for thermal ageing out-of-pile. One measure of the degree of segregation is the loss of energy as time evolves. For the Fe–20Cr potential we see an energy loss in the system corresponding to 85% of the mixing enthalpy. This is perfectly consistent with the surface to bulk relation of 30% in this system considering that half the neighbours of the surface atoms are Fe atoms. For the Fe–5Cr we should not see any energy loss at all since the potential predicts a negative mixing enthalpy. As can be seen in Fig. 3 we have a clear segregation of Cr atoms in a system of 20% Cr after a simulated month at 800 K. The time scale is in very good agreement with experiments on 45% Cr at 770 K [32].

## 4. Summary and Conclusions

The set of EAM potentials for Fe–Cr alloys under development yield activation energies for vacancy migration in the pure elements that are in very good agreement with experimental data. The predicted SIA formation energies arising from fitting to thermal expansion coefficients are higher than values obtained by other authors using both EAM and ab initio methods. While electron irradiation data seems to support lower numbers, the stored energy release measured in neutron-irradiated samples is compatible with our results.

Applied to simulation of thermal ageing, there is no sign of precipitation taking place when using the potential fitted to the negative formation energy previously calculated for ferromagnetic Fe–5Cr. KMC simulations using the potential fitted to the mixing enthalpy of Fe–20Cr yield formation of Cr clusters on a time and temperature scale that is in good agreement with measurements of hardening in high Cr binary alloys.

We predict that the  $\langle 110 \rangle$  Fe–Cr and Cr–Cr dumbbells are more stable than the corresponding defect in pure iron. Consequently, Cr would tend to end up in defect structures forming during the cooling down of recoil cascades.

### Acknowledgements

The authors would like to thank B. Singh, D. Bacon and Y. Osetsky for inspiring discussions and the following institutions for financial support: The Swedish Research council (P.O. I.A.A.), the EU 5th FP project SPIRE (R.C.), Svensk Kärnbränslehantering AB (J.W.) and Svenskt Kärntekniskt Centrum (C.L.).

### References

- [1] J. Wallenius, P. Olsson, C. Lagerstedt, N. Sandberg, R. Chakarova, V. Pontikis, *Phys. Rev. B* 69 (2004) 094103.
- [2] P. Olsson, I.A. Abrikosov, L. Vitos, J. Wallenius, *J. Nucl. Mater.* 321 (2003) 84.
- [3] M.S. Daw, M.I. Baskes, *Phys. Rev. B* 29 (1984) 6440.
- [4] A.F. Voter, Principles, in: J.H. Westbrook, R.L. Fleischer (Eds.), *Intermetallic Compounds*, vol. 1, Wiley, 1995.
- [5] J. Rose, J. Smith, J. Ferrante, *Phys. Rev. B* 28 (1983) 1835.
- [6] F. Nix, D. MacNair, *Phys. Rev.* 60 (1941) 597.
- [7] G. White, R. Roberts, E. Fawcett, *J. Phys. F* 16 (1986) 449.
- [8] S. Burke, R. Cywinski, J. Davies, B. Rainford, *J. Phys. F* 13 (1983) 451.
- [9] J.P. Biersack, J.F. Siegler, *Nucl. Instrum. and Meth.* 141 (1982) 93.
- [10] D. Farkas, C.G. Schon, M.S.F. de Lima, H. Goldstein, *Acta Mater.* 44 (1996) 409.
- [11] O. Yifang, Zh. Bangwei, L. Shuzhi, J. Zhanpeng, *Z. Phys. B* 101 (1996) 161.
- [12] C.S. Becquart, C. Domain, A. Legris, J.-C. van Duysen, *J. Nucl. Mater.* 280 (2000) 73.
- [13] P. Olsson, L. Malerba, A. Almazouzi, SCKCEN Report, BLG-950, June 2003.
- [14] C. Domain, private communication, 2004.
- [15] G. Ackland, D.J. Bacon, A.F. Calder, T. Harry, *Philos. Mag. A* 75 (1997) 713.
- [16] J.A. Rayne, B.S. Chandrasekar, *Phys. Rev.* 122 (1961) 1714.
- [17] W. Bendick, W. Pepperhof, *Acta Metall.* 30 (1982) 679.
- [18] M. Lübbehusen, H. Mehrer, *Acta Metall. Mater.* 38 (1990) 283.
- [19] A. Seeger, *Phys. Stat. Sol. A* 167 (1998) 289.
- [20] L. De Schepper, D. Segers, L. Dorikens-Vanpraet, M. Dorikens, G. Knuyt, L.M. Stals, P. Moser, *Phys. Rev. B* 27 (1983) 5257.
- [21] C.C. Fu, Proceedings of ITEM Technical Workshop WP2, 2003.
- [22] P. Moser, *Mem. Sci. Rev. Metall.* 63 (1966) 431.
- [23] H. Bilger, V. Hivert, J. Verdone, J.L. Leveque, J.C. Soulie, *Int. Conf. on Vacancies and Interstitials in Metals*, Kernforschungsanlage Jülich, 1968, p. 751.
- [24] H. Wollenberger, in: R. Chan, P. Haasen (Eds.), *Physical Metallurgy*, vol. 2, North-Holland, 1996.
- [25] P. Vajda, *Rev. Mod. Phys.* 49 (1977) 481.
- [26] P. Erhart, *Mater. Res. Soc. Symp.* 41 (1985) 13.
- [27] K.W. Katahara, M. Nimalendran, M.H. Manghnani, E.S. Fischer, *J. Phys. F* 9 (1979) 2167.
- [28] H. Schultz, *Mater. Sci. Eng. A* 141 (1991) 149.
- [29] G.D. Loper, L.C. Smedskjaer, M.K. Chason, R.W. Siegel, in: P. Jain, R. Singru, K. Gopinathan (Eds.), *Positron Annihilation*, World Scientific, 1985, p. 461.
- [30] R. Fischer, E. Dulis, K. Carrol, *Trans. AIME* 197 (1953) 690.
- [31] H. Kuwano, *Trans. JIM* 26 (1985) 473.
- [32] J. Hyde, M. Miller, A. Cerezo, G. Smith, *Appl. Surf. Sci.* 87&88 (1995) 311.